Al_3O_y (y=0–5) clusters: Sequential oxidation, metal-to-oxide transformation, and photoisomerization

Cite as: J. Chem. Phys. **109**, 449 (1998); https://doi.org/10.1063/1.476583
Submitted: 26 February 1998 . Accepted: 31 March 1998 . Published Online: 29 June 1998

Hongbin Wu, Xi Li, Xue-Bin Wang, Chuan-Fan Ding, and Lai-Sheng Wang

Al_3O_y ($y=0-5$) clusters: Sequential oxidation, metal-to-oxide transformation, and photoisomerization

Hongbin Wu, Xi Li, Xue-Bin Wang, Chuan-Fan Ding, and Lai-Sheng Wang[a)]
Department of Physics, Washington State University, 2710 University Drive, Richland, Washington 99352-1671 and W. R. Wiley Environmental Molecular Sciences Laboratory, Pacific Northwest National Laboratory, MS K8-88, P.O. Box 999, Richland, Washington 99352

(Received 26 February 1998; accepted 31 March 1998)

Photoelectron spectra of a series of $Al_3O_y^-$ clusters ($y=0-5$) are presented at several photon energies: 532, 355, 266, and 193 nm. The electron affinities and low-lying electronic states of the Al_3O_y clusters are reported. The photoelectron spectra clearly reveal a sequential oxidation behavior and how the electronic structure of the clusters evolves from that of a metal cluster at Al_3 to that of a complete oxide cluster at Al_3O_5: Two valence electrons of Al_3 are observed to be transferred to each additional O atom until Al_3O_5, where all the nine valence electrons of Al_3 are transferred to the five O atoms. The anion, $Al_3O_5^-$, which can be viewed as $(Al^{3+})_3(O^{2-})_5$, is found to be a closed shell cluster, yielding an extremely high electron affinity for Al_3O_5 (4.92 eV). The electron affinities of the remaining clusters are: 1.90 (Al_3), 1.57 eV (Al_3O), 2.18 eV (Al_3O_2), 2.80 eV (Al_3O_3), and 3.58 eV (Al_3O_4). An electronic excited state of Al_3^- is also observed at 0.40 eV above the Al_3^- ground state. Isomers are observed for all the oxide clusters with lower electron affinities. Particularly, vibrational structures are observed for the two isomers of $Al_3O_3^-$, as well as a photoisomerization process between the two isomers. The structure and bonding of the oxide clusters are discussed based on the experimental data and the known structures for Al_3 and Al_3O.
 [S0021-9606(98)01026-5]

I. INTRODUCTION

The interaction between oxygen and aluminum is known to be mainly of ionic character.[1] In bulk Al_2O_3, the valence electrons of Al are transferred to the O atoms, giving the insulating property of the bulk oxide material: The valence and conduction bands of Al_2O_3 are composed mainly of O2p and Al3p, respectively, with a large band gap. The Al and O atoms can be approximately described as Al^{3+} and O^{2-} in the bulk, whose cohesive energies derive primarily from the electrostatic interactions. Such ionic interactions are expected in the small Al and O molecules and Al_xO_y clusters. For a series of Al_xO_y clusters with fixed x ($y=0$ to bulk composition), one expects the electronic structure of the Al_xO_y clusters to become increasingly simple because the valence electrons of Al are sequentially transferred to the O atoms. By studying these clusters, one not only obtains microscopic information of the oxidation of a cluster, but also follows the transformation from a metal to an oxide cluster, or a molecular metal-to-nonmetal transition. In this article, we study a series of $Al_3O_y^-(y=0-5)$ clusters, using anion photoelectron spectroscopy (PES) which shows directly how the valence electrons of the Al_3 clusters are transferred to O with each O addition until $Al_3O_5^-$ in which all the ten valence electrons (nine from Al plus the extra charge) are transferred to O. In addition, we have observed a second isomer for $Al_3O_y^-(y=1-4)$ and photoisomerization between the two isomers of $Al_3O_3^-$.

Al_3 has been well studied in the past and is known to be a nearly equilateral triangle with a doublet ($^2A_1$) ground state.[2–8] Al_3O has been studied theoretically as an example of hypermetalated species,[9,10] but no theoretical studies of the higher Al_3O_y clusters have appeared. Experimentally, there have been many studies of the small aluminum oxide clusters.[11,12] However, few studies have been carried out for the larger aluminum oxide clusters except for a few mass spectrometric works.[13–17] Therefore, little is known about the Al_3O_y clusters (for $y>1$) investigated presently. Our main research interests concern the microscopic investigation of the structure and chemical bonding of small oxide clusters and the potential application of the oxide clusters as microscopic models to understanding bulk oxide surfaces and defects. We have studied a number of oxide systems, including Si,[18–21] Ge,[22] Ti,[23] Fe,[24–27] Cu,[28–30] and V oxides[31] and the smaller Al oxide clusters[11,12] and have observed sequential oxidation behaviors in these systems.

In the current work, we present a systematic PES study of the $Al_3O_y^-(y=0-5)$ series at several photon energies: 532 nm (2.331 eV), 355 nm (3.493 eV), 266 nm (4.661 eV), and 193 nm (6.424 eV), including vibrationally resolved spectra for $Al_3O_3^-$. We show that the electron affinity (EA) of the neutral Al_3O_y species increases with the O content and the valence PES spectra of the $Al_3O_y^-$ species become simpler with increasing y because the valence electrons of the Al are transferred to the O atoms. The PES spectra show that two electrons from the Al_3 clusters are in fact transferred to each O atom to make O^{2-}, resulting in a very high EA for Al_3O_5 which is one electron short of the ten electrons needed for the five O atoms. In addition, isomers have been ob-

a)Author to whom correspondence should be addressed.

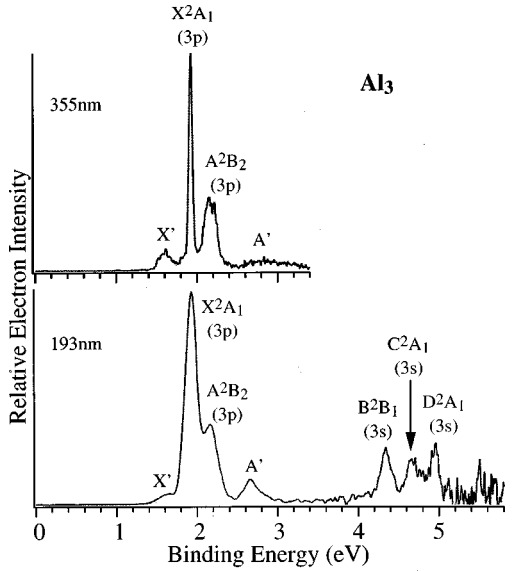

FIG. 1. Photoelectron spectra of Al_3^- at 355 and 193 nm.

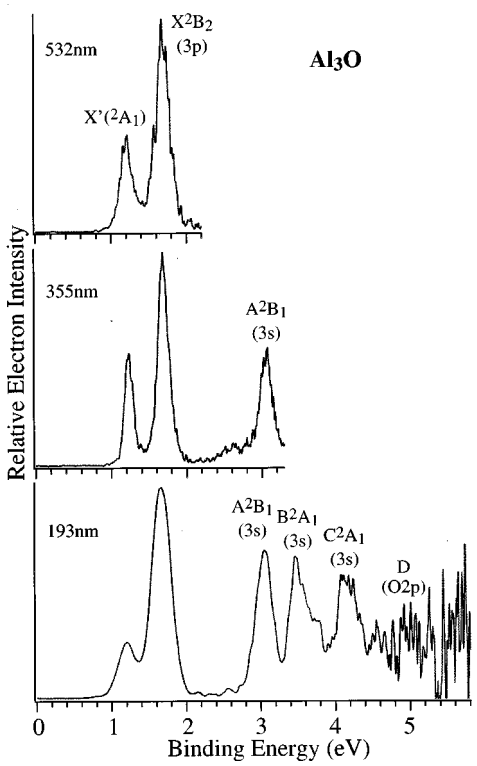

FIG. 2. Photoelectron spectra of Al_3O^- at 532, 355, and 193 nm.

served for all the oxide clusters. Surprisingly, a photoisomerization between the two isomers of $Al_3O_3^-$ was observed under high detachment laser fluences. Based on the experimental observations and the known structures of Al_3 and Al_3O, possible structures of the higher oxide clusters are proposed and discussed.

II. EXPERIMENT

The experimental apparatus used in this work has been described in detail elsewhere.[32,33] Briefly, it consists of a laser vaporization supersonic cluster source, a time-of-flight (TOF) mass spectrometer, and a magnetic-bottle TOF photoelectron analyzer. A pure Al disk target, positioned by two computer-controlled stepping motors, was vaporized by the second harmonic of a Nd:YAG laser (5–20 mJ/pulse). An intense helium carrier gas pulse was delivered to the target by two Jordan valves (10 atm backing pressure) and synchronized with the vaporization event. To produce oxide clusters, we seeded the He carrier gas with various amounts of O_2 ranging from 0.05%–5%. Usually, a low O_2 concentration favors generation of clusters with less oxygen content. For Al_3O^-, in fact, no oxygen seeding in the He carrier gas was necessary. The oxide layer on the Al target surface was sufficient to produce abundant Al_3O^- signals. For very small clusters, particularly, diatomic oxide molecules, we found that we could vary the cluster temperature significantly, depending on the timing between the vaporization event and the arrival of the He carrier gas. If the vaporization laser is fired too early relative to the arrival of the carrier gas, very hot negative ions would be produced. In this condition, no large clusters could be produced, and the molecular anions were mostly from the surface contamination. If the laser vaporization event was timed with the peak of the carrier gas pulse, colder anions were produced. However, the latter condition often produced smaller molecular anions with reduced abundance due to collisional loss or rapid cluster growth that consumed the smaller anions.

The oxide clusters were entrained in the carrier gas and underwent a supersonic expansion. After being collimated by a skimmer, the anion clusters were extracted from the cluster beam perpendicularly and sent into a TOF mass analyzer. The desired clusters were mass selected and decelerated before being intercepted by a detachment laser beam in the interaction zone of the magnetic-bottle TOF photoelectron analyzer. A variety of detachment laser wavelengths were used, including the three harmonics of a Nd:YAG laser (532, 355, and 266 nm) and an ArF excimer laser (193 nm). Low photon energies yielded better resolved spectra for low binding energy features whereas high photon energies allowed more tightly bonded electrons to be detached. However, significant noise existed at high photon energies (above 266 nm, 4.661 eV) where low photon fluences were used and shot-to-shot background subtraction had to be done. The 532 and 355 nm spectra were all taken at 10 Hz repetition rate whereas the 266 and 193 nm spectra were taken at 20 Hz with the vaporization laser off at alternating shots for the background subtraction. The photoelectrons emitted in all 4π solid angles were collected by the magnetic-bottle and analyzed in a 3.5 m long TOF tube. Photoelectron TOF spectra were averaged for $1-3\times10^4$ laser shots and were converted to electron kinetic energy spectra calibrated using the known spectrum of Cu^-. The binding energy spectra presented were obtained by subtracting the kinetic energy spectra from the detachment photon energies. The resolution of the spectrometer was better than 30 meV FWHM for 1 eV electrons and deteriorated for high electron kinetic energies.

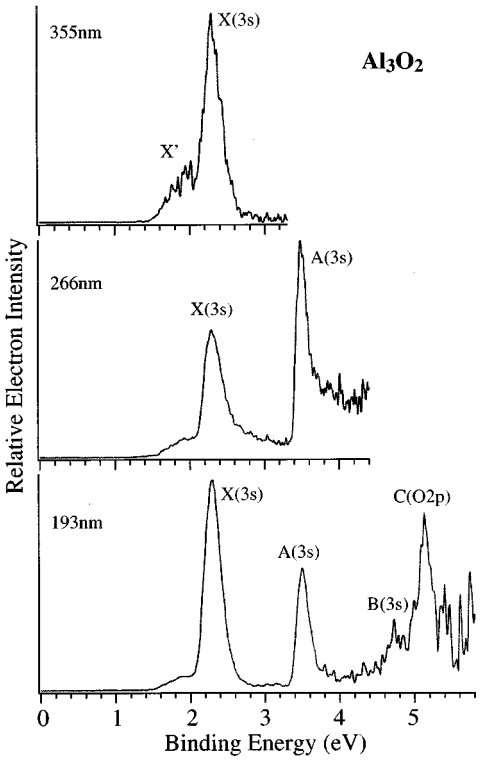

FIG. 3. Photoelectron spectra of $Al_3O_2^-$ at 355, 266, and 193 nm.

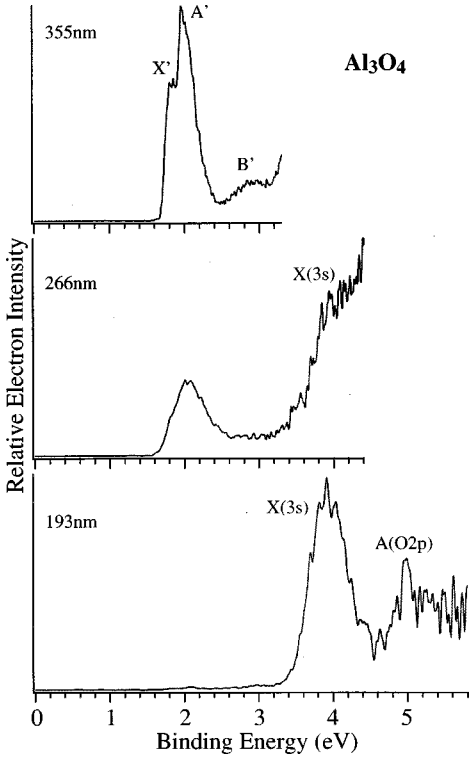

FIG. 5. Photoelectron spectra of $Al_3O_4^-$ at 355, 266, and 193 nm. Note the decreased intensity of the X', A', and B' at 193 nm, indicating they are from a minor isomer.

III. RESULTS

Photoelectron spectra of $Al_3O_y^-(y=0-4)$ at various photon energies are shown in Figs. 1–5, respectively. The spectrum of $Al_3O_5^-$, only measured at 193 nm due to its high electron binding energy, is given in Fig. 6 and compared with the 193 nm spectra of all the other species. The spectra of Al_3^- were taken at two photon energies and a total of seven detachment features were observed as shown in Fig. 1. The binding energies of the detachment features for Al_3^- are given in Fig. 7, along with the detailed spectral assignments which will be discussed in the following section. The spectra of Al_3O^-, measured at three photon energies, are displayed in Fig. 2. Five distinct features were observed and more transitions exist around 5 eV as can be seen in the 193 nm spectrum, but the poor signal-to-noise ratio prevents us from making any definitive assignments of the high binding energy features. The $Al_3O_2^-$ spectra at three photon energies are given in Fig. 3 which reveals four distinct spectral features and a weak low energy feature (X'). The $Al_3O_3^-$ cluster was also investigated at three photon energies as shown in Fig. 4. Vibrational structures were clearly resolved in the two spectral features at 355 nm, as indicated in Fig. 4 by the vertical lines. Two more features were observed at the higher photon energy spectra of $Al_3O_3^-$. The spectra of $Al_3O_4^-$, obtained at three photon energies, are shown in Fig. 5. These spectra show some unusual behavior: The low energy features (X', A', and B') observed in the low photon energy spectra seemed to disappear in the 193 nm spectrum where only two broad features (X and A) were observed. Close examination of the 193 nm spectrum reveals that the low energy features still exist, but at much lower intensity barely above the baseline. The $Al_3O_5^-$ cluster exhibits very high electron binding energies and its photoelectron spectrum could only be measured at 193 nm as given in Fig. 6. The spectrum of $Al_3O_5^-$ also shows a low energy tail, recognizable down to about 3.5

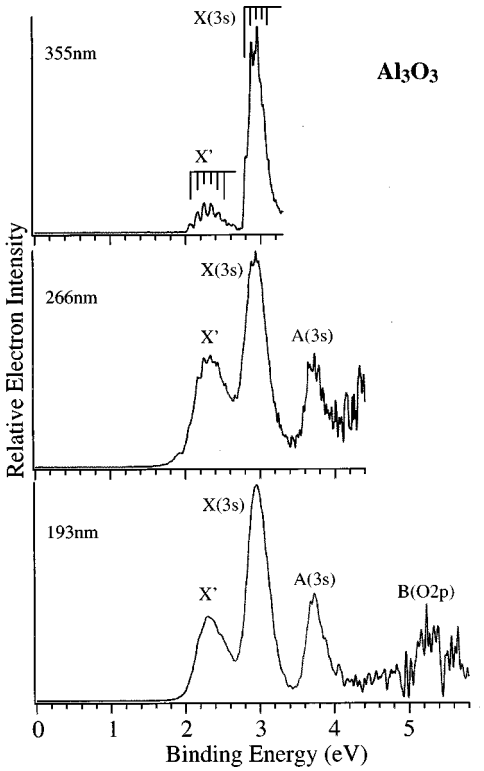

FIG. 4. Photoelectron spectra of $Al_3O_3^-$ at 355, 266, and 193 nm. The vertical lines indicate the resolved vibrational structure.

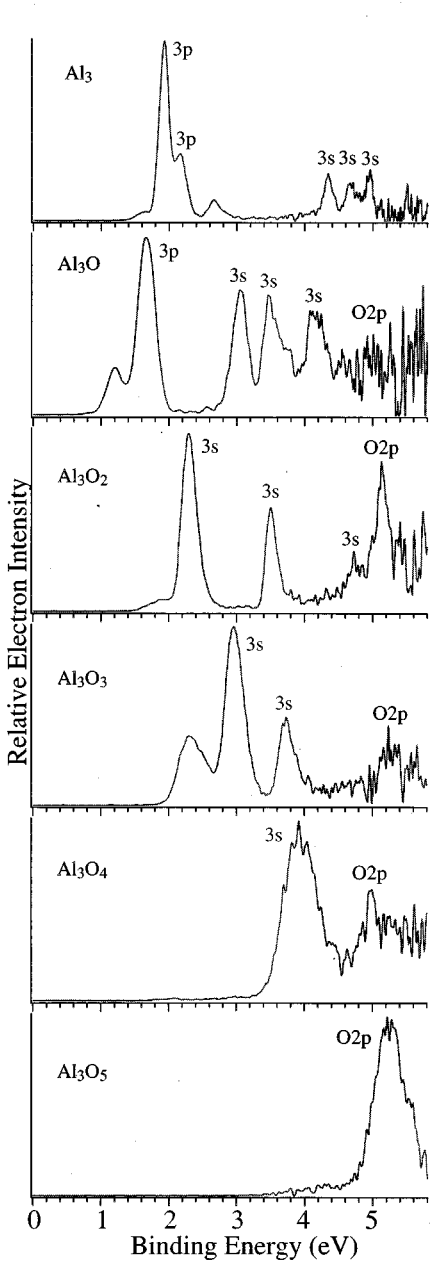

FIG. 6. Comparison of the 193 nm spectra of $Al_3O_y^-$, $y=0-5$.

eV. We tried to measure the $Al_3O_5^-$ spectrum at 266 nm (4.661 eV) photon energy in order to resolve the tail, but did not observe any useful spectral features except for a smooth tail resembling the tail in the 193 nm spectrum. The binding energies of all the observed spectral features for $Al_3O_y^-$ ($y=1-5$) are given in Table I.

The unusual behavior observed in the $Al_3O_4^-$ spectra suggests that there were different isomers populated in the cluster beam. The low binding energy features (Fig. 5, X', A', and B') should be due to a minor isomer and only the 193 nm spectrum revealed the dominating isomer. In fact, we observed isomers for Al_3O^-, $Al_3O_2^-$, and $Al_3O_3^-$, as well: The lowest binding energy feature (labeled as X') in the spectra of these species (Figs. 2–4) was due to a minor isomer. The weak low energy tail in the $Al_3O_5^-$ spectrum was also likely to be due to a minor isomer in the cluster beam.

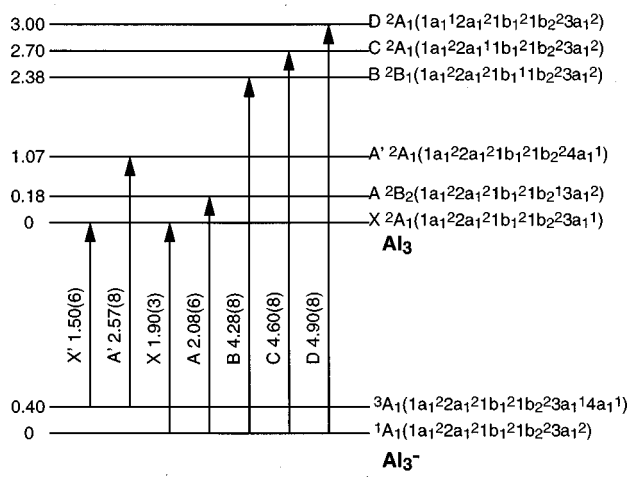

FIG. 7. Observed detachment transitions and their binding energies, and the low-lying energy levels and their electron configurations of the Al_3O^- and Al_3O. The binding energies and excited state energies are in eV.

The isomers for $Al_3O_2^-$ and $Al_3O_3^-$ are made very clear in Figs. 8 and 9, where the minor isomer populations were shown to vary significantly with experimental conditions. The electron affinities observed in the current work for all the isomers are summarized in Table II. The detailed spectral assignments are discussed in the following section.

IV. DISCUSSION

The photoelectron spectra shown in Figs. 1–6 represent detachment transitions from the anions to the various states of the neutral clusters, i.e., the low-lying energy levels of the neutral clusters. However, except for Al_3 which has been subjected to several previous experimental and theoretical

TABLE I. Observed binding energies (BE) of the energy levels for Al_3O_x ($x=1-4$) and isomers.

	BE (eV)	Term value (eV)
Al_3O		
$X\ ^2B_2\ (3a_1^2 4a_1^2 2b_1^2 2b_2^1)$	1.57 (6)	0
$A^2B_1\ (3a_1^2 4a_1^2 2b_1^1 2b_2^2)$	2.95 (6)	1.38
$B\ ^2A_1\ (3a_1^2 4a_1^1 2b_1^2 2b_2^2)$	3.48 (8)	1.91
$C\ ^2A_1\ (3a_1^1 4a_1^2 2b_1^2 2b_2^2)$	4.08 (8)	2.51
$X'(Y)$	1.14 (6)	0
Al_3O_2		
X	2.18 (6)	0
A	3.44 (5)	1.36
B	4.65 (10)	2.47
C	5.08 (8)	2.90
X'	1.6 (1)	0
Al_3O_3		
X	2.80 (2)	0
A	3.60 (5)	0.80
B	5.1 (1)	2.3
X'	2.07 (2)	0
Al_3O_4		
X	3.58 (8)	0
A	5.10 (9)	1.52
X'	1.75 (6)	0
A'	1.91 (8)	0.16
B'	(2.6)	(0.9)

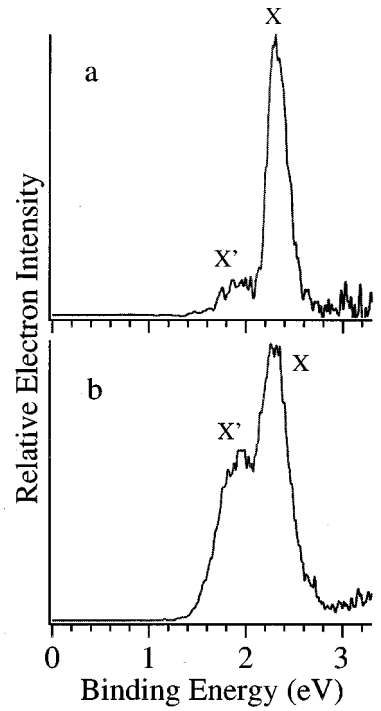

FIG. 8. Photoelectron spectra of $Al_3O_2^-$ at 355 nm under two source conditions, showing the two isomeric forms of $Al_3O_2^-$. (a) Using a pure He carrier gas; (b) using a 0.5% O_2/He carrier gas.

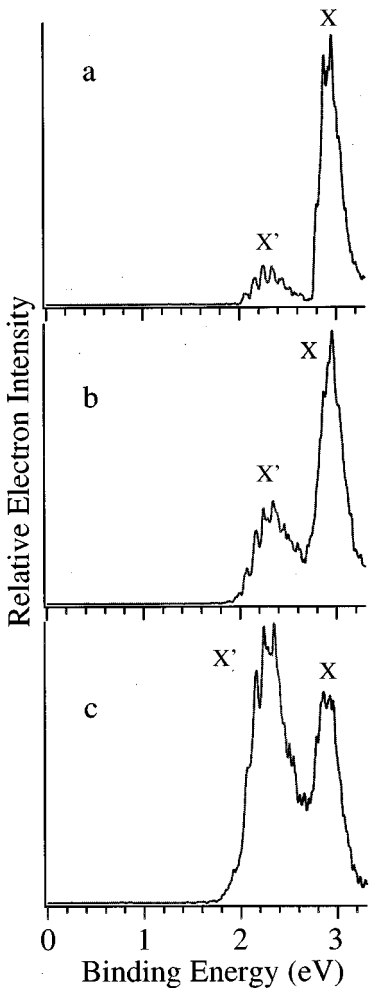

FIG. 9. Temperature and detachment laser fluence dependence of the photoelectron spectra of $Al_3O_3^-$ at 355 nm, showing two isomeric forms and their photoisomerization. (a) Taken at cold source condition; (b) taken at hotter source condition—isomer X' is enhanced (laser fluence, 0.8 mJ/pulse, 3 mm dia. spot size); (c) same as (b), laser fluence, 3 mJ/pulse.

investigations[2–8] and Al_3O for which there have been two previous theoretical studies,[9,10] there have been no experimental or theoretical studies about the oxide clusters for Al_3O_2 to Al_3O_5. Our discussion begins with Al_3 and Al_3O for which quantitative assignments are possible based on the molecular orbital and structural information available from the previous theoretical investigations. We then will give a qualitative discussion for the higher oxide clusters with the help of the geometrical and electronic structure information of Al_3 and Al_3O.

A cursory observation of the spectra presented in Fig. 6 shows that the spectra seem to become simpler with increasing O content. The electron binding energies are seen to increase with the O content, as well. Both of these effects are indications of a sequential electron transfer of the valence electrons from Al_3 to each additional O atom, which has a higher electron binding energy (high electron affinity). The spectral simplicity of all the $Al_3O_y^-$ clusters is also due to a fortunate electron counting (even number of valence electrons) which is likely to lead to closed shell ground state for all the anions. Closed shell anions usually give simpler spectra because detachment of each occupied orbital will only lead to one detachment feature (a doublet final neutral state) in the single particle approximation and in the absence of spin–orbit splitting. For example, for an open shell anion with one unpaired electron, detachment of a fully occupied molecular orbital will always lead to a singlet and a triplet neutral state. The valence electron configuration of Al is $3s^2 3p^1$ with three valence electrons and that of O is $2s^2 2p^4$. Therefore, the total number of valence electrons in all the neutral Al_3O_y clusters is an odd number whereas the anions with one extra electron all have even number of electrons. In bulk Al_2O_3, the three valence electrons are transferred to the O atoms, giving Al^{3+} and O^{2-} closed shell ions.[1] If we assume that a similarly ionic bonding picture holds in the Al_3O_y clusters, then the valence electrons will decrease from nine in Al_3 by two for each O addition, until Al_3O_5 which is

TABLE II. Observed adiabatic electron affinity (EAa), and vertical electron affinity (EAv), and vibrational frequency of Al_3O_x ($x=0-5$) and their observed isomers.[a]

Cluster	EAa (eV)	EAv (eV)	Vib. freq. (cm^{-1})
Al_3	1.90 (3)	1.90 (3)	
Al_3O (T)	1.57 (6)	1.68 (5)	
Al_3O_2	2.18 (6)	2.29 (6)	
Al_3O_3	2.80 (2)	2.96 (2)	610 (60)
Al_3O_4	3.58 (8)	3.92 (8)	
Al_3O_5	4.92 (8)	5.21 (8)	
Al_3O (Y)[a]	1.14 (6)	1.22 (5)	
Al_3O_2 (iso)[a]	1.6 (1)	1.9 (1)	
Al_3O_3 (iso)[a]	2.07 (2)	2.25 (2)	720 (60)
Al_3O_4 (iso)[a]	1.75 (6)	1.81 (6)	

[a]See Table I, Figs. 2–5, 8, and 9, and the text for isomer assignments.

one electron short, thus leading to a very high electron binding energy for $Al_3O_5^-$ which is a perfectly closed shell anion. This qualitative picture seems to agree well with the photoelectron spectra observed for Al_3O_y. The fact that we have not been able to observe an $Al_3O_6^-$ anion with any substantial abundance is also consistent with this qualitative bonding picture.

A. Al_3/Al_3^- and excited state of Al_3^-

Several theoretical calculations have been carried out on Al_3 and its electronic and geometrical structure is well understood.[2–5] Al_3 has a C_{2v} symmetry with a nearly equilateral triangle structure. Its valence molecular orbital can be described as: $1a_1^2 2a_1^2 1b_1^2 1b_2^2 3a_1^1$ with a $^2A_1$ ground state, where the $1a_1$, $2a_1$, and $1b_1$ are mainly the Al3s orbitals, the $1b_2$ and $3a_1$ are a π and σ orbital, respectively, derived from the Al3p orbitals.[2] The highest occupied molecular orbital of Al_3 in the D_{3h} symmetry would be a doublet degenerate orbital ($2e'$). Thus Al_3 cannot possess the D_{3h} symmetry due to the Jahn–Teller effect. In Al_3^-, the extra electron enters the $3a_1$ orbital, giving a $^1A_1$ ground state for the anion ($1a_1^2 2a_1^2 1b_1^2 1b_2^2 3a_1^2$). The extra electron can also enter the $4a_1$ orbital, giving a triplet excited state of Al_3^-: $^3A_1$ ($1a_1^2 2a_1^2 1b_1^2 1b_2^2 3a_1^1 4a_1^1$), which was calculated to be 0.40 eV above the ground state.[2] The photoelectron spectra shown in Fig. 1 can be definitively assigned based on the above electronic structure information.

The weak features labeled as X' and A' depended on experimental conditions, but they could not be completely eliminated. These features were also observed in two previous PES experiments.[7,8] They can be either due to an Al_3^- isomer or excited state of Al_3^-. We assign them as due to the excited state of Al_3^-. Then the intense and sharp feature labeled X should represent the ground-to-ground state transition. The energy difference between the X' and X features would represent the excitation energy of Al_3^-, as shown in Fig. 7. The 0.40 eV excitation energy we obtained is in excellent agreement with the previous calculation for the $^3A_1$ excited state of Al_3^-, supporting our assignment of the X' feature. The A' feature then represents detachment of the $3a_1$ electron from the excited state anion, leading to a $^2A_1$ excited state of neutral Al_3 ($1a_1^2 2a_1^2 1b_1^2 1b_2^2 4a_1^1$) as shown in Fig. 7.

The five major features in Fig. 1, X, A, B, C, and D, are then due to detachment from the ground state of Al_3^- ($1a_1^2 2a_1^2 1b_1^2 1b_2^2 3a_1^2$), corresponding to removal of an electron from the $3a_1$, $1b_2$, $1b_1$, $2a_1$, and $1a_1$ orbitals, respectively. The assignments are given in Fig. 1 and the detailed energy levels observed currently are shown schematically in Fig. 7. Therefore, there is a one-to-one correspondence between the detachment transitions and the occupied molecular orbitals of Al_3^-. Such spectral simplicity can only arise when the anion is closed shell, and in the absence of multielectron transitions, spin–orbit splittings, or degenerate orbitals. The $X\ ^2A_1$ ground state feature is very sharp with little indication of vibrational excitation, suggesting that there is little geometry change between the ground state of the anion and that of the neutral. It is also interesting to note that the three transitions (B, C, and D) from the three Al3s-type orbitals are fairly close in energy. The binding energies of these three transitions are also very similar to that of the Al3s in Al^- (4.1 eV).[34] Both of these observations suggest that the 3s orbitals in the trimer are quite localized and the bonding interactions in Al_3 come primarily from the 3p orbitals. This is not surprising since the 3s-to-3p promotion energy in Al atom is 3.6 eV,[35] which is rather high compared to the Al–Al bonding energy. In a recent study,[34] we have shown that the $3s-3p$ hybridization increases with cluster size and the 3s- and 3p-derived orbitals become completely overlapped only at Al_9.

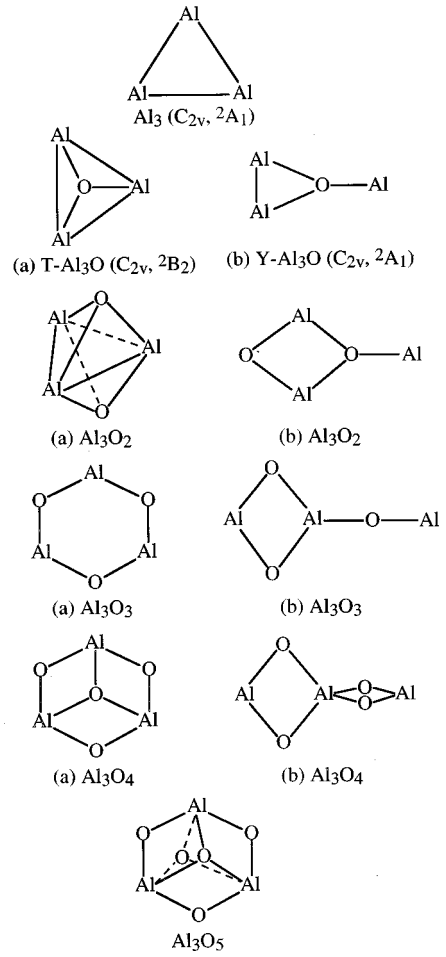

FIG. 10. Suggested structures for the Al_3O_y clusters. The structure of Al_3 is from Ref. 2 and the structure of Al_3O is from Ref. 9.

B. Al_3O/Al_3O^- and isomers

Al_3O has been investigated in two previous theoretical studies as an example of a class of so-called hypermetallic molecules, i.e., metal-rich molecules in which the valence of the metals exceeds that of the non-metal elements.[9,10] Several structures of Al_3O were considered and the lowest energy structure was identified as a T-type geometry with a C_{2v} symmetry, which is schematically shown in Fig. 10. Another Y-type isomer, also shown in Fig. 10, was only 0.5 kcal/mol higher in energy. Other isomers calculated were all considerably higher in energy. The T-type isomer, which should be predominantly produced in our experiment, has a $^2B_2$ ground state with the following configuration:

$1a_1^2 2a_1^2 1b_2^2 1b_1^2 3a_1^2 4a_1^2 2b_1^2 2b_2^1$, where the $1a_1$ orbital is the O2s, the $2a_1$, $1b_2$, and $1b_1$ orbitals are derived primarily from the O2p, the $3a_1$, $4a_1$, and $2b_1$ orbitals are mainly of Al3s character, and the $2b_2$ orbital is mainly of Al3p character.[9] In the anion, the extra electron should enter the $2b_2$ orbital, yielding a closed shell singlet ground state, $^1A_1$. The uppermost valence molecular orbital configuration of Al_3O is therefore quite similar to that of Al_3 discussed above, except that two Al3p electrons are transferred to a predominantly O2p orbital. Our observed photoelectron spectra can be interpreted using the above theoretical information.

The photoelectron spectra of Al_3O^- are shown in Fig. 2 at three photon energies. Two features were observed in the 532 nm spectrum with partially resolved vibrational structures. The 355 nm spectrum revealed a new feature at around 3 eV and two more major features were observed in the 193 nm spectrum at around 3.5 and 4.2 eV. More features exist at higher binding energies in the 193 nm spectrum, but they cannot be definitively identified due to the poor signal-to-noise ratio. We found that the intensity ratio between the lowest binding energy feature (X') and the strong feature at 1.6 eV (X) could be varied slightly under different experimental conditions: The intensity of the X' feature was slightly enhanced when the clusters were produced at a hotter condition, suggesting that the weaker X' feature is either due to an excited state of Al_3O^- or a different isomer. We assign the X' feature to be due to the Y-type isomer and the main features to the T-type isomer identified in the previous theoretical calculations as the global minimum. The ground state of the Y-type isomer was a doublet state ($^2A_1$), as shown in Fig. 2. The weak features between 2.4–2.8 eV, observed more clearly in the 355 nm spectrum, were also likely to be due to the Y-type isomer. However, we will focus mainly on the T isomer.

The X feature is then the ground state of Al_3O, arising from detachment from the Al3p-type $2b_2$ orbital. The A, B, and C features are assigned to be from detachment of the three Al3s-type orbitals, $2b_1$, $4a_1$, and $3a_1$, respectively. The features around 5 eV or higher are probably due to the O2p-type orbitals, whose binding energies are known to be high. For example, the binding energies of the O2p-type orbitals in $Al_2O_y^-$ clusters were observed to be around 5 eV or higher.[12] Therefore, the main features of the Al_3O^- spectra are all due to Al. The seemingly similarity of the Al_3O^- spectrum to that of Al_3^-, as shown more clearly in Fig. 6, lends support to our assignment. Both the T and Y isomers have three totally symmetric vibrational modes, which may all be active, preventing us from observing a simple vibrational progression in the 532 nm spectrum in Fig. 2. Our resolution was not sufficient to allow us to determine vibrational frequencies which would be useful to compare with the calculated values for the two isomers. However, the electron affinities of the two isomers are quite different and were determined fairly accurately (see Table II), which will be interesting to compare with future calculations. We have shown previously that experimentally measured adiabatic and vertical electron affinities are valuable parameters to compare to theoretical calculations to distinguish isomers and determine cluster structures.[18,21,22,29]

C. $Al_3O_2/Al_3O_2^-$ and isomers

The spectra of $Al_3O_2^-$ were measured at three photon energies and are shown in Fig. 3. The 355 nm spectrum shows an intense band (X) at about 2.3 eV and a weaker broad feature (X') at lower binding energy. At 266 nm, one additional feature was observed at about 3.5 eV and the 193 nm spectrum revealed two more features (B and C) at about 4.7 and 5.1 eV, respectively. The weak feature (X') was shown to depend on source conditions. The spectra shown in Fig. 3 were all taken with low O_2 concentration (0.05%–0.1% O_2 in He). Figure 8 shows two spectra of $Al_3O_2^-$ taken at 355 nm under two very different source conditions. The spectrum in Fig. 8(a) was taken with pure He carrier gas. Under this condition, small amount of $Al_3O_2^-$ could be generated with a fresh target surface, and we observed that the intensity of the X' feature was very low. Figure 8(b) shows a spectrum taken at higher O_2 concentration (0.5%) in the He carrier gas and the intensity of the X' feature was enhanced considerably. However, we could not eliminate the X' feature completely. The dramatic dependence on the source conditions suggests that the X' feature was due to another minor isomer of $Al_3O_2^-$. Therefore, we assign the four main features (X, A, B, and C) to be due to the major isomer.

From Al_3 to Al_3O, essentially two valence electrons of Al_3 are transferred to the O atom, as discussed above. Similarly, in Al_3O_2, two more electrons are expected to be donated to the extra O atom, leaving only five valence electrons on Al_3. In the anion, there will be six electrons occupying mainly the three Al3s orbitals. As we have seen above, the O2p derived orbitals have high binding energies around 5 eV or higher. Thus, we assign the feature at 5.1 eV to be due to the O2p-derived orbitals and the three lower energy features to be from the Al3s-type orbitals. Compared to Al_3O^-, the three Al3s-derived features are more separated (Fig. 6).

It would be interesting to speculate about the possible structures of the two isomers observed in our experiment. Two candidates can be suggested based on the two isomers observed for Al_3O^-, as shown in Fig. 10. The structure (a), a trigonal bipyramid, is suggested based on the T-type isomer of Al_3O. Structure (b) is based on the Y-type isomer of Al_3O by adding the second O to the Al–Al bond. Without accurate theoretical calculations, we cannot comment on the relative stability of either isomer. However, the structure (a), in which the two O atoms are equally bonded to the three Al, may be expected to be more stable and could correspond to the major isomer in our experiment.

D. $Al_3O_3/Al_3O_3^-$: isomers and photoisomerization

We measured the photoelectron spectra of $Al_3O_3^-$ at three photon energies (Fig. 4). Two vibrationally resolved bands (X' and X) were observed at 355 nm detachment energy. We obtained a vibrational frequency for the X' band to be about 720 cm^{-1}. The X band is more complicated with at least two active modes. The higher frequency mode yielded a vibrational spacing of about 610 cm^{-1}, and the lower frequency mode is about 300–350 cm^{-1}, which was not well resolved. The 266 nm spectrum revealed a new feature at about 3.7 eV. At 193 nm, another feature at about 5.2 eV

was further observed. The intensity of the X' band seemed to be enhanced significantly at the higher detachment photon energies.

We found that the intensity of the X' band actually depended on our source conditions. The 355 nm spectrum shown in Fig. 4 was taken at a much colder source condition. Figure 9(b) shows a 355 nm spectrum of $Al_3O_3^-$ at a slightly higher source temperature by firing the vaporization laser earlier relative to the He carrier gas. Compared to the cold spectrum of $Al_3O_3^-$ [Fig. 9(a)], the intensity of the X' feature under the hot condition was considerably increased, implying that the X' feature was due to a different isomer. More surprisingly, when the detachment laser fluence was increased, the intensity of the X' band was dramatically increased, as shown in Fig. 9(c). The source conditions for the spectra of Figs. 9(b) and 9(c) were the same except that the laser fluence used for Fig. 9(c) was about four times higher than that used for Fig. 9(b). This suggests that the two isomer populations were in fact altered by the detachment laser intensity. This is a clear example of photoisomerization. Somehow the anions of the isomer due to X, which is probably lower in energy, absorbed a photon and then isomerized to another structure due to X'. Photoabsorption by anions and subsequent relaxation to internal energies were first observed in a photodetachment experiment of C_{60}^-,[36] and have since been observed in photodetachment experiments of many metal cluster anions, causing low electron energy tails in photoelectron spectra due to thermionic emission.[37] However, this is the first time that photoisomerization has ever been observed in an anion system.

Therefore, we attribute the three main features (X, A, and B) to the major isomer. The feature B at 5.2 eV should be due to detachment from the O2p-type orbitals as in Al_3O^- and $Al_3O_2^-$. The X and A features are then assigned to be from detachment of the Al3s-type orbitals. Compared to $Al_3O_2^-$, two more valence electrons are transferred to the third O in $Al_3O_3^-$. Thus only two features were expected from the two pairs of electrons in the Al3s-type orbitals.

Even though vibrational information was obtained for the two isomers of Al_3O_3, their structures were still not known without accurate theoretical calculations. Two suggestions were made as shown in Fig. 10. The ring structure (a) in which each O is bonded to two Al was expected to be more stable and should be a reasonable candidate for the major isomers observed in our experiment. We found previously that Si_3O_3 has a similar ring-type structure.[20,21] The structure (b) might be a good candidate for the X' isomer, which is similar to the (b) isomer of Al_3O_2.

E. $Al_3O_4/Al_3O_4^-$ and isomers

The spectra of $Al_3O_4^-$, measured at three photon energies, are shown in Fig. 5. The 355 nm spectrum showed three features. The X' and A' features were overlapping and the B' feature was rather broad. The 266 nm spectrum revealed more features at high binding energies, but were very broad. Surprisingly, the 193 nm spectrum showed only two broad features (X and A) at high binding energies. The lower binding energy features seemed to disappear in the 193 nm spectrum. However, close examination of the 193 nm spectrum suggested that the low binding energy features were still there, but with extremely weak intensities, suggesting that the low binding energy features were all from a minor isomer of $Al_3O_4^-$.

We again assign the high binding energy feature around 5 eV to be due to detachment from O2p-type orbitals. In Al_3O_4, only one valence electron is left on the Al_3, probably occupying a Al3s-type orbital. In the anion, the extra electron paired up with this electron, giving the broad detachment feature at about 3.8 eV. Two structures were suggested for the isomers of Al_3O_4, as shown in Fig. 10. The structure (a), formed by adding the fourth O to the structure (a) of Al_3O_3, might be a reasonable candidate for the main isomer we observed because all the Al atoms are equivalent in this structure and there are more Al–O bonds. The structure (b), comprised of two Al_2O_2 rhombuses, was suggested as a candidate for the other isomer observed in our experiment. This structure was suggested based on the Si_3O_4 cluster which we have determined definitively to be a D_{2d} structure with two perpendicular Si_2O_2 rhombuses.[18,20,21] The central Si in this case is tetra coordinated, similar to the environment in bulk silica. Although in bulk Al_2O_3, Al is coordinated by six O, the Al in aluminosilicate is four coordinated, similar to the structure (b) suggested for Al_3O_4 in Fig. 10.

F. $Al_3O_5/Al_3O_5^-$: A complete oxide cluster

$Al_3O_5^-$ has a very high electron binding energy and its photoelectron spectrum could only be measured at 193 nm photon energy, which is shown in Fig. 6. A low energy tail was seen in the 193 nm spectrum of $Al_3O_5^-$, possibly due to isomers. We measured the spectrum of $Al_3O_5^-$ at 266 nm to examine the low energy tail, but did not obtain any useful information. Only a broad tail was observed. The high binding energy of the detachment feature of $Al_3O_5^-$ suggests that it is due to detachment of the O2p-type orbitals. The lack of lower energy features indicates that all the valence electrons of Al_3 are transferred to the O atoms in $Al_3O_5^-$. Indeed, just from the electron counting, the nine valence electron of Al_3 plus the extra electron of the anion would make $Al_3O_5^-$ a perfect closed shell anion, consistent with its high binding energy. Therefore, in $Al_3O_5^-$, all the Al atoms can be viewed as Al^{3+} and all the O atoms as O^{2-}, making $Al_3O_5^-$ a complete oxide molecule, similar to the bulk oxide. Figure 10 shows a suggested structure for this cluster, which is formed by adding the fifth O atom to that of the structure (a) of Al_3O_4. In this structure, the three Al atoms are surrounded by the five O atoms, a favorable arrangement from a simple electrostatic consideration. Another isomer of Al_3O_5 may be considered by adding the fifth O atom to one of the terminal Al atom in structure (b) of Al_3O_4, a structure similar to Si_3O_5.[21] However, only one isomer was dominate as indicated from our photoelectron spectrum of $Al_3O_5^-$.

G. Sequential oxidation, structural evolution, and the nature of ionic bonding in the Al_3O_y clusters

Figure 6 compares all the photoelectron spectra of $Al_3O_y^-$ ($x=0-5$) at 193 nm detachment energy. Several in-

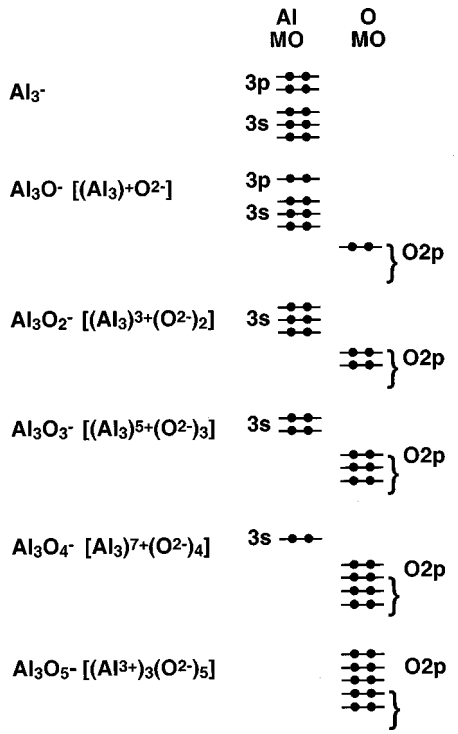

FIG. 11. Schematic molecular orbital (MO) representation of electron transfers from Al to O in the $Al_3O_y^-$ ($y=0-5$) series of clusters. Note that not all the orbitals derived from O2p are shown.

teresting points can be made and deserve further discussion. If we just consider those features from the main isomers as labeled, we see a clear trend of sequential oxidation and transition from a metal cluster (Al_3) to an oxide cluster (Al_3O_5). The spectral features derived from the Al3s, Al3p, and O2p are labeled in Fig. 6, which shows how two valence electrons of Al_3 are sequentially transferred to the O atom at each oxidation step, until all the valence electrons of Al_3 are transferred to the O atoms in Al_3O_5. Figure 11 shows a schematic representation of the electron transfers from Al to O in the $Al_3O_y^-$ clusters. This series of clusters may be viewed as true molecular analogs of how an Al surface is oxidized with increasing O atom adsorption until the formation of bulk Al_2O_3 oxide.[38]

The electron affinities observed for the clusters (Table II) are shown to increase with the O content except for the first step from Al_3 to Al_3O. This trend is similar to that observed previously for Fe_3O_y and Fe_4O_y series of clusters, where we used a simple electrostatic model to rationalize the trend of the electron affinity with increasing O content in the clusters.[27] We considered the metal cluster as a sphere with a radius (R). A net charge transfer (δ) occurs from the metal cluster to the O atom upon each O adsorption. Then a simple electrostatic consideration could qualitatively account for the electron affinity increase with the O content. This simple model seems to apply to the Al_3O_y $[(Al_3)^{+y\delta}(O^{-\delta})_y]$ series of clusters. The only constraint in the model is that the O atoms are adsorbed on the surface of the metal clusters. The structures of the main isomers (a) for the Al_3O_y ($x=2-5$) shown in Fig. 10 were proposed to be consistent with this simple idea of sequential O atom chemisorption on the cluster surface. The near linear increase of the electron affinity with the O content provides some indirect support for these proposed structures. Of course, these are very simple considerations, and accurate theoretical calculations will be required to determine definitively the cluster structures. The experimental data presented in this work, i.e., electron affinities, low-lying electronic energy levels, vibrational frequencies (Al_3O_3 only), and isomeric information, should prove valuable for future theoretical studies. However, the ionic bonding nature between Al and O, i.e., charge transfers from Al to O are shown very clearly from the current data.

Another noteworthy observation is that the binding energies of the O2p-derived orbitals appear to be similar in all the $Al_3O_y^-$ clusters (Fig. 6). This was also true for the $Al_2O_y^-$ series of clusters.[12] It is interesting to note that the binding energy of the O2p (O^{2-}) in bulk Al_2O_3 happens at about 5 eV below the Fermi level, i.e., the valence band edge, which is entirely composed of the O2p orbitals.[1,38] The binding energy of the O2p in the $Al_xO_y^-$ clusters occurs almost in the same energy range, further evidence suggesting that the O atoms in these oxide clusters can be viewed as O^{2-} similar to the bulk oxide. This observation is consistent with our experimental data and provides additional evidence for the ionic nature of the bonding between Al and O in the $Al_xO_y^-$ clusters.

V. CONCLUSIONS

We report a comprehensive photoelectron spectroscopic investigation of $Al_3O_y^-$ ($x=0-5$) at various photon energies. Electron affinities and low-lying electronic structure information were obtained for all the clusters. An excited state of the Al_3^- anion was observed and assigned based on previous theoretical calculations. A second isomer was observed for all the oxide clusters and electron affinities were obtained for all the isomers. In particular, a surprising photoisomerization was observed between the two isomers of $Al_3O_3^-$. The systematic data allowed us to observe atom-by-atom how the electrons of Al are transferred to O in the Al_3O_y clusters at each O addition, i.e., a sequential oxidation. Essentially we have observed a metal (Al_3) to nonmetal (Al_3O_5) transition in a finite system since $Al_3O_5^-$ emulates a complete oxide cluster with all the valence electrons of Al transferred to the O atoms. Therefore, the ionic bonding nature between Al and O was directly probed. Based on the two known isomers of Al_3O and the nature of the sequential oxidation, possible structures of the higher oxide clusters were proposed and discussed. The current series of clusters provides true molecular analogs of the oxidation of aluminum surfaces and warrants further theoretical investigations.

ACKNOWLEDGMENTS

This work is supported by the U.S. Department of Energy, Office of Basic Energy Sciences, Chemical Sciences Division and is conducted at the Pacific Northwest National Laboratory, operated for the U.S. Department of Energy by Battelle under Contract DE-AC06-76RLO 1830. L.S.W. is an Alfred P. Sloan Research Fellow.

[1] V. E. Henrich and P. A. Cox, *The Surface Science of Metal Oxides* (Cambridge University Press, New York, 1994).
[2] H. Basch, Chem. Phys. Lett. **136**, 289 (1987).
[3] R. O. Jones, J. Chem. Phys. **99**, 1194 (1993).
[4] L. G. M. Pettersson, C. W. Bauschlicher, Jr., and T. Halicioglu, J. Chem. Phys. **87**, 2205 (1987).
[5] T. H. Upton, Phys. Rev. Lett. **56**, 2168 (1986); J. Chem. Phys. **86**, 7054 (1987).
[6] Z. Fu, G. W. Lemire, Y. M. Hamrick, S. Taylor, J. C. Shui, and M. D. Morse, J. Chem. Phys. **88**, 3524 (1988).
[7] K. J. Taylor, C. L. Pettiette, M. J. Craycraft, O. Chesnovsky, and R. E. Smalley, Chem. Phys. Lett. **152**, 347 (1988).
[8] C. Y. Cha, G. Gantefor, and W. Eberhardt, J. Chem. Phys. **100**, 995 (1994).
[9] A. I. Boldyrev and P. R. Schleyer, J. Am. Chem. Soc. **113**, 9045 (1991).
[10] V. G. Zakrzewski, W. von Niessen, A. I. Boldyrev, and P. R. Schleyer, Chem. Phys. **174**, 167 (1993).
[11] S. R. Desai, H. Wu, and L. S. Wang, Int. J. Mass Spectrom. Ion Processes **159**, 75 (1996).
[12] S. R. Desai, H. Wu, C. Rohfling, and L. S. Wang, J. Chem. Phys. **106**, 1309 (1997), and references therein.
[13] Z. Liu, C. Wang, R. Huang, and L. Zheng, Int. J. Mass Spectrom. Ion Processes **141**, 201 (1995).
[14] D. M. Cox, D. J. Trevor, R. L. Whetten, E. A. Rohlfing, and A. Kaldor, J. Chem. Phys. **84**, 4651 (1986).
[15] M. F. Jarrold and J. E. Bower, J. Chem. Phys. **85**, 5373 (1986); **87**, 5728 (1987).
[16] S. A. Ruatta, L. Hanley, and S. L. Anderson, Chem. Phys. Lett. **137**, 5 (1987).
[17] F. L. King, B. I. Dunlap, and D. C. Parent, J. Chem. Phys. **94**, 2578 (1991).
[18] J. Fan, J. B. Nicholas, J. M. Price, S. D. Colson, and L. S. Wang, J. Am. Chem. Soc. **117**, 5417 (1995).
[19] L. S. Wang, H. Wu, S. R. Desai, J. Fan, and S. D. Colson, J. Phys. Chem. **100**, 8697 (1996).
[20] L. S. Wang, S. R. Desai, H. Wu, and J. B. Nicholas, Z. Phys. D **40**, 36 (1997).
[21] L. S. Wang, J. B. Nicholas, M. Dupuis, H. Wu, and S. D. Colson, Phys. Rev. Lett. **78**, 4450 (1997).
[22] J. B. Nicholas, J. Fan, H. Wu, S. D. Colson, and L. S. Wang, J. Chem. Phys. **102**, 8277 (1995).
[23] H. Wu and L. S. Wang, J. Chem. Phys. **107**, 8221 (1997).
[24] J. Fan and L. S. Wang, J. Chem. Phys. **102**, 8714 (1995).
[25] L. S. Wang, J. Fan, and L. Lou, Surf. Rev. Lett. **3**, 695 (1996).
[26] H. Wu, S. R. Desai, and L. S. Wang, J. Am. Chem. Soc. **118**, 5296 (1996).
[27] L. S. Wang, H. Wu and S. R. Desai, Phys. Rev. Lett. **76**, 4853 (1996).
[28] H. Wu, S. R. Desai, and L. S. Wang, J. Chem. Phys. **103**, 4363 (1995).
[29] L. S. Wang, H. Wu, S. R. Desai, and L. Lou, Phys. Rev. B **53**, 8028 (1996).
[30] H. Wu, S. R. Desai, and L. S. Wang, J. Phys. Chem. A **101**, 2103 (1997).
[31] H. Wu and L. S. Wang, J. Chem. Phys. **108**, 5310 (1998).
[32] L. S. Wang, H. S. Cheng, and J. Fan, J. Chem. Phys. **102**, 9480 (1995).
[33] L. S. Wang and H. Wu, in *Advances in Metal and Semiconductor Clusters*, edited by M. A. Duncan (JAI Press, Greenwich, 1998), Vol. 4, pp. 299–343.
[34] X. Li, H. Wu, X. B. Wang, and L. S. Wang, Phys. Rev. Lett. (submitted).
[35] C. E. Moore, *Atomic Energy Levels*, Natl. Bur. Stand. Circ. (U.S. GPO, Washington, D.C. 1971), Vol. I.
[36] L. S. Wang, J. Conceicao, C. Jin, and R. E. Smalley, Chem. Phys. Lett. **182**, 5 (1991).
[37] G. Gantefor, W. Eberhardt, H. Weidele, D. Kreisle, and E. Recknagel, Phys. Rev. Lett. **77**, 4524 (1996), and references therein.
[38] H. D. Ebinger and J. T. Yates, Jr., Phys. Rev. B **57**, 1976 (1998).